International Journal of Microwave and Wireless Technologies, 2013, 5(1), 35–42.
doi:10.1017/S1759078712000694

RESEARCH PAPER

Angular measurements in azimuth and elevation with 77 GHz radar sensors

KLAUS BAUR, MARCEL MAYER, STEFFEN LUTZ AND THOMAS WALTER

An antenna concept for direction of arrival estimation in azimuth and elevation is proposed for 77 GHz automotive radar sensors. This concept uses the amplitude information of the radar signal for the azimuth angle and the phase information for the elevation angle. The antenna consists of a combination of a series-fed-array structure with a cylindrical dielectric lens. This concept is implemented into a radar sensor based on SiGe MMICs for validation. A two- and a four-beam configuration are presented and discussed with respect to angular accuracy and ambiguities.

Keywords: Antenna design, Modeling and measurements, Radar applications

Received 29 May 2012; Revised 5 October 2012

I. INTRODUCTION

77 GHz radar sensors are considered as key components for advanced driver assistance systems. Especially, the availability of SiGe technology with transit frequencies exceeding 200 GHz [1] enabled the development of highly integrated transceivers for automotive applications [2]. In combination with innovative packaging concepts such as eWLB [3], cost effective radar sensors, fulfilling the demands of a high volume production, and the associated quality requirements were demonstrated and introduced in the market [4]. Based on this monolithic microwave integrated circuit (MMIC) technology, innovative radar sensors for advanced safety functions in all vehicle classes were developed and demonstrated in the project RoCC.

This transition from sole comfort functions (e.g. ACC – adaptive cruise control) to safety functions such as advanced emergency braking systems (AEBS) in order to mitigate or even avoid accidents is accompanied by enhanced specifications with respect to the detection and localization of objects in the surrounding environment of a car. A major aspect addressed in future radar generations will be the estimation of the elevation angle of an object in addition to the azimuth angle. Thus, the driver assistance system will be able to instantly classify the detected objects into relevant obstacles and non-relevant objects such as a beverage can on the road. In this contribution, an antenna concept consisting of the combination of a planar antenna array and a cylindrical dielectric lens for the angular estimation in azimuth and elevation is presented and discussed. This antenna concept was implemented into a 77 GHz automotive radar sensor based on SiGe MMICs and evaluated with respect to the angular accuracy by correlation algorithms.

Institute for Medical Engineering and Mechatronics, University of Applied Sciences Ulm, Albert-Einstein-Allee 55, 89081 Ulm, Germany
Corresponding author:
K. Baur
Email: klausbaur@gmx.de

II. ANTENNA CONCEPT

The antenna concept for angular measurements in azimuth and elevation is based on amplitude information for the azimuth angle and on phase information for the elevation angle. For a two-beam configuration, a phase monopulse and amplitude monopulse principle could be applied for the direction of arrival (DOA). However, as the system was extended to a four-beam configuration, correlation methods [5] for the DOA were chosen for both antenna configurations. A similar concept was proposed by Hausz and Zachery [6] based on a parabolic reflector and dipole antennas in the X-band. Alternative concepts for future automotive radar generations with angular measurement capabilities in elevation are presented in [7]. Figure 1 shows our antenna concept based on a planar antenna array and a cylindrical dielectric lens. The cylindrical dielectric lens with an effective aperture width D and a length L is mounted in front of at least two feed antennas A1 and A2 with lateral offsets d_x and d_y with respect to each other. In this monostatic radar configuration, these two antennas transmit and receive signals. In a later stage, two additional receive antennas were added to the system in order to widen the field of view and to improve the angular measurement performance (Section VI). As pointed out above, the amplitude information is used for angular estimation in the azimuth, whereas the phase information is used in the elevation. In the azimuth (H-plane) the displacement d_x of the two antennas leads to a beam squint as a consequence of the quasi-optical beamforming imposed by the cylindrical dielectric lens enabling the use of the amplitudes (Fig. 2(a)). In the elevation (E-plane) angular measurements based on the phase difference between two antennas can be carried out due to a displacement d_y of the antennas (Fig. 2(b)). With respect to the elevation no optical beamforming is performed by the lens since it only acts as a kind of dielectric cover. Therefore, distortions of the phase difference should be low.

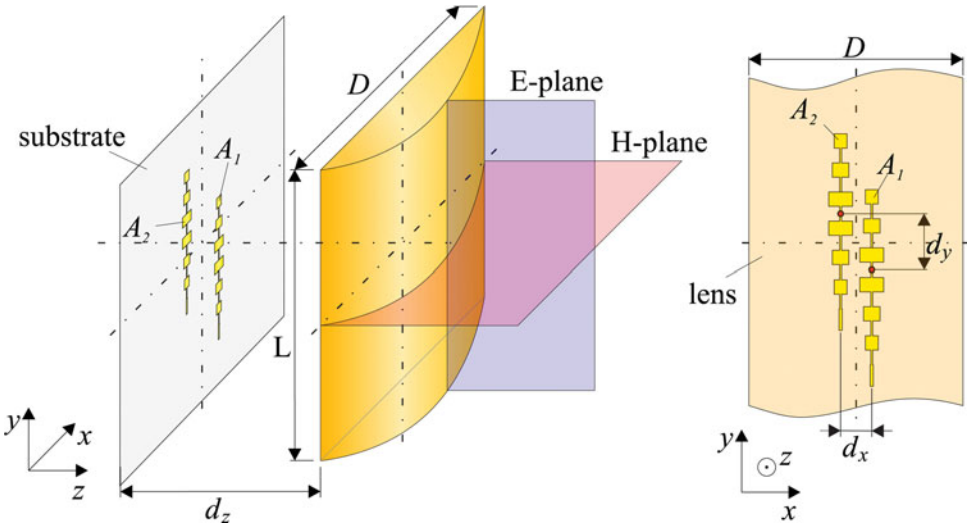

Fig. 1. Concept with two series fed arrays and a cylindrical dielectric lens.

As no optical beamforming occurs in the *E*-plane the amplitude ratio of the two beams is independent of the elevation angle which is the most important precondition for the application of an amplitude mono-pulse with respect to the estimation of the azimuth angle. Furthermore, for the application of a phase mono-pulse principle for the elevation angle, the phase difference must be independent of the azimuth angle in the overlap region of the two beams. However, fulfilling this criterion is more challenging. Simulations and measurements clearly revealed that this criterion strongly depends on the distance between the antennas and the lens surface. In [8], it was shown that in the vicinity of the nominal focal plane the phase difference becomes independent of the azimuth angle of the incident wave. Thus, the distance between the antennas and the lens surface is a critical parameter with respect to the performance of our antenna concept. Furthermore, a lens with two refracting surfaces was chosen, having the advantage that it will not refocus surface reflections back to the feeding element [9]. However, in order to cope with phase distortions due to standing waves between the lens surface and the back plane of the RF substrate [10] an antireflective coating was emulated using a grooved dielectric layer in accordance with the design rules given in [11]. Such a concept is advantageous with respect to a conventional quarter wave transformer as no low-loss material with a specific refractive index is required. In addition, spherical aberrations were accounted for by an aspherical shape of the lens surface [12]. Polyetherimid, a low-loss thermoplastic material with a permittivity of 3.04 at 76 GHz was selected for the lens.

As described above, the dielectric lens is illuminated by a planar antenna array. Since no optical beamforming occurs in the *E*-plane by the dielectric lens, the desired beam width has to be adjusted by the aperture of the planar antenna array. A series-fed-array design was chosen due to a less complex and more compact feed line network exhibiting low losses and a reduced parasitic radiation. Figure 3 shows a series-fed-array antenna with six elements as utilized in our concept. In order to keep the side-lobe level low a tapered linear antenna configuration was developed on a Rogers 3003 substrate with a permittivity ε_r of 2.96 at 76 GHz and a thickness h of 127 μm.

III. SENSOR CONCEPT

A) Architecture

In order to evaluate our concept the antenna configuration described above was implemented into a commercial radar

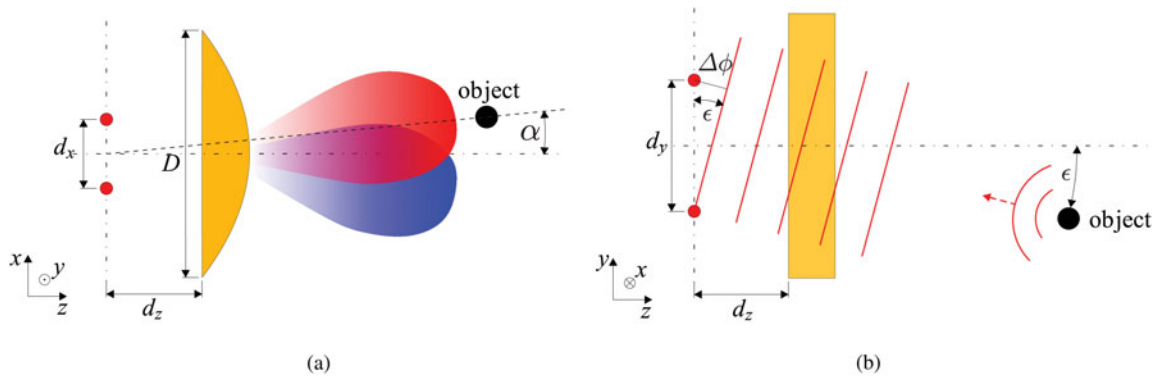

Fig. 2. Concept for angular estimations in azimuth and elevation: (a) azimuth. (b) elevation.

https://doi.org/10.1017/S1759078712000694 Published online by Cambridge University Press

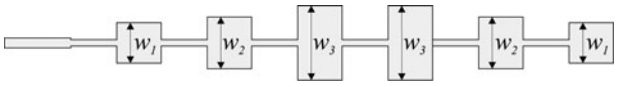

Fig. 3. Series-fed array antenna.

sensor [13]. A key component of the sensor is a SiGe-four-channel radar transceiver with two transceiving channels and two receiving channels (Fig. 4) [2]. As shown in Fig. 5(a) the radar sensor consists of two separate blocks, an RF-module and a control unit. The RF-module contains the 77 GHz transceiver which is mounted in a cavity in the substrate directly onto a heat sink core. In addition, a 19 GHz DRO reference oscillator being part of a phase-locked loop (PLL) (Radar-ASIC) reduces the phase noise of the 77 GHz oscillator and facilitates frequency-modulated continuous wave (FMCW) modulation. The antennas are placed on the RF-substrate and connected via bondwires directly to the SiGe-MMIC.

Figure 5(b) exhibits a photograph of the developed prototype which was used for the measurements discussed in the following sections. A dielectric lens with an aperture width of $D = 30$ mm and a focal length of $f = 25$ mm is used in combination with a metal housing (size $77 \times 74 \times 49$ mm^3) of the sensor enabling an efficient heat transfer.

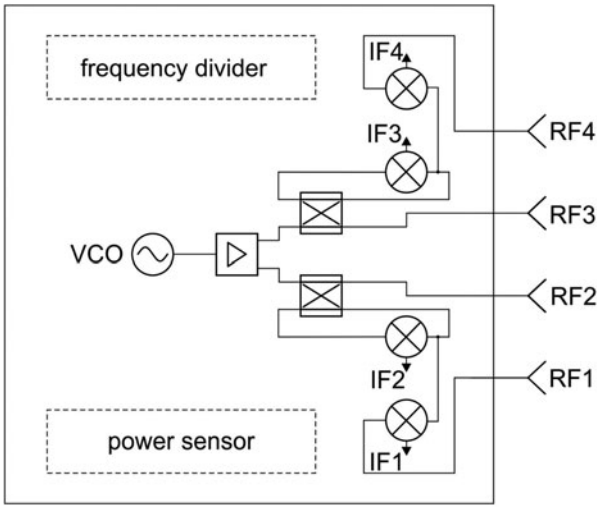

Fig. 4. MMIC architecture.

B) Measurement results

Figure 6 shows the measured antenna characteristic of the sensor with both antennas transmitting simultaneously in phase (*E*- and *H*-planes) in comparison with the simulated results. The 3 dB beam width accounts for 13.2° in the *E*-plane (Fig. 6(a)) and 7.0° in the H-plane (Fig. 6(b)). The measured transmit characteristics show a side-lobe suppression of −12.7 dB in the *H*-plane and of −19.7 dB in the *E*-plane. Simulated and measured results are in good agreement with only minor differences in the side-lobe suppression. These differences can be attributed to the fact that the housing of the sensor and the frame of the lens were not included in the simulations (CST-Microwave Studio). One-and two-way measurements were performed in an anechoic chamber. The radar sensor therefore is mounted on a two-dimensional rotational stage. For the two-way measurements, a corner reflector with an radar cross section (RCS) of 54 m^2 at a distance of 5 m was used as reference target. A ramp duration of 5 ms and a bandwidth of 500 MHz with a center frequency of 76.5 GHz was chosen for the FMCW modulation.

IV. SYSTEM EVALUATION

A) Two channel configuration

In this section, the receive characteristics of the two-channel sensor and the impact of defocusing the lens system on the angular measurement will be discussed. In the receive case, both antennas receive the signal separately. For the defocused case, the distance between the antennas and the lens surface was increased by 4 mm with respect to the focal length. As mentioned above, a significant impact on the phase difference in the *H*-plane could be expected from defocusing the lens system [8]. Figure 7(a) shows the simulated receive characteristics in the *E*-plane. In order to be consistent with the four-channel system which will be discussed below the two channels in the two-channel configuration are labeled IF2 and IF3. As no optical beamforming is performed in this plane, the antenna diagram of the two beams is almost identical with only a minor influence of defocusing the lens system. Figure 7(b) contains the receive characteristics in the *H*-plane exhibiting a beam squint due to the optical beamforming in this plane. Again, a defocusing of the lens system causes only minor changes with respect to the main lobes, however, leads to an increased side-lobe level. The phase

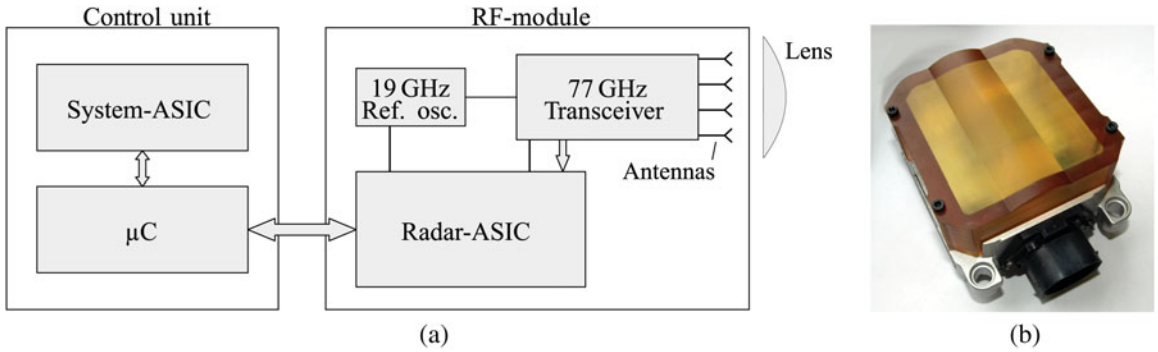

Fig. 5. Architecture and housing of the prototype: (a) block diagram and (b) prototype.

https://doi.org/10.1017/S1759078712000694 Published online by Cambridge University Press

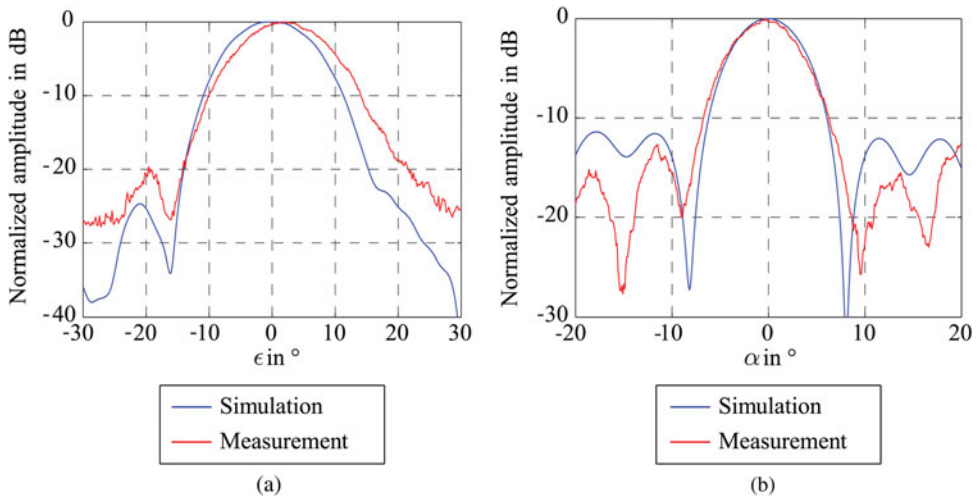

Fig. 6. Measured and simulated antenna pattern in the (a) *E*- and (b) *H*-plane.

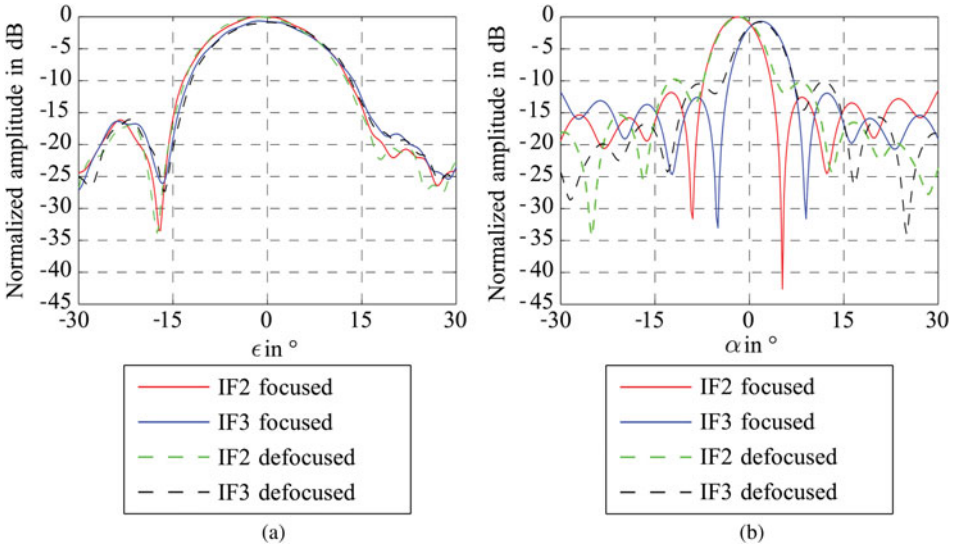

Fig. 7. Simulated RX-characteristics for the focused and defocused case: (a) *E*-plane. (b) *H*-plane.

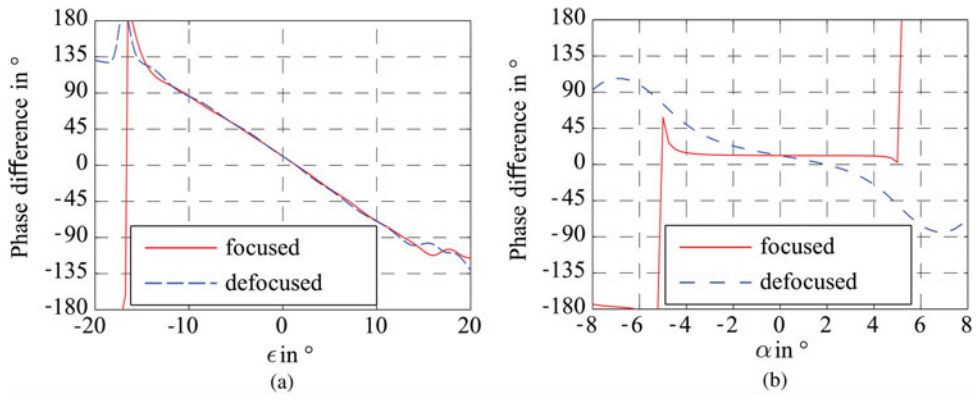

Fig. 8. Simulated phase difference for the focused and defocused case: (a) *E*-plane and (b) *H*-plane.

https://doi.org/10.1017/S1759078712000694 Published online by Cambridge University Press

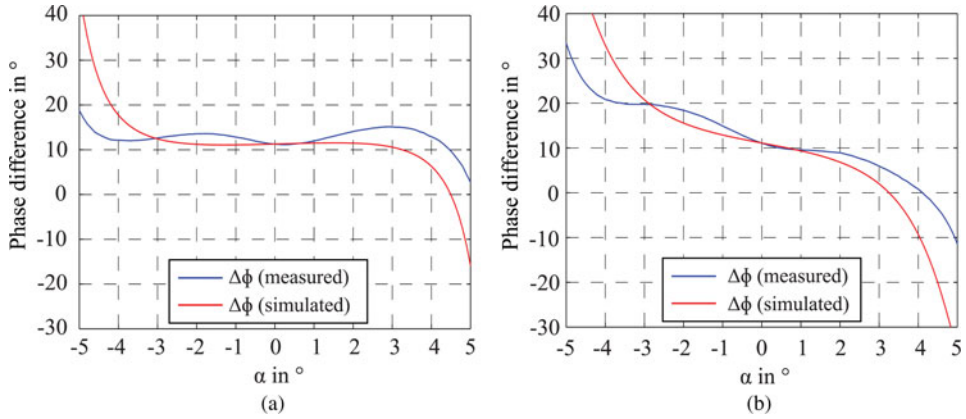

Fig. 9. Simulated and measured phase differences for the (a) focused and (b) defocused case.

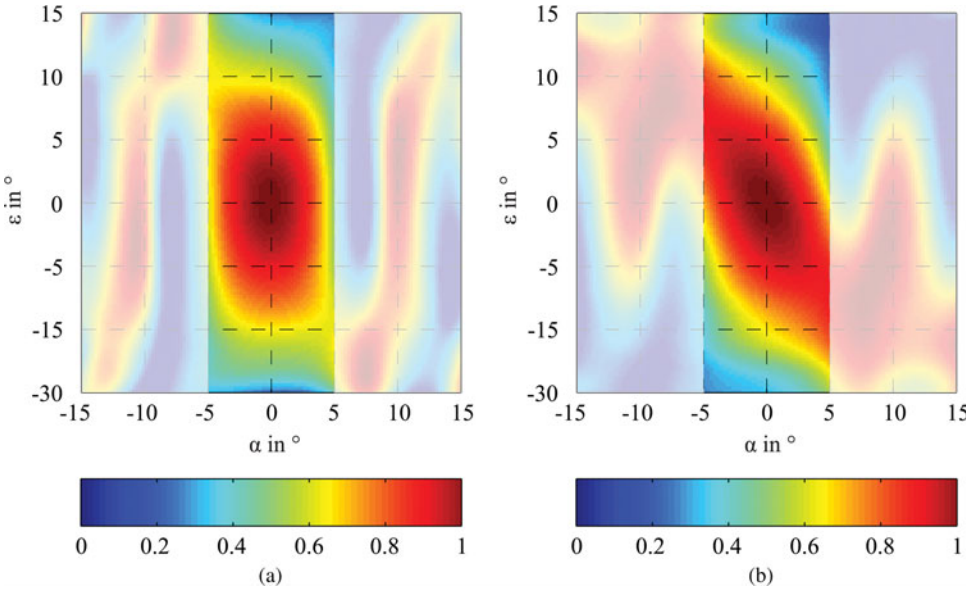

Fig. 10. Autocorrelation diagram for the (a) focused and (b) defocused case with two beams.

difference in the *E*-plane (Fig. 8(a)) exhibits very linear characteristics not being affected by the defocusing of the lens system, whereas with respect to the *H*-plane a severe impact on the phase difference can be observed from Fig. 8(b). As requested for our concept mounting the antennas in the focal plane leads to a quite constant phase difference (Fig. 9(a)) while defocusing results in a gradient of the phase difference (Fig. 9(b)) [14]. Thus, for the defocused case both the elevation angle and the azimuth angle of an object result in a phase difference and consequently in ambiguities.

In order to determine the angular accuracy and possible ambiguities, correlation algorithms have been applied as described in [5]. This method also accounts for coupling phenomena of adjacent antennas as the correlation is performed based on a steering vector which includes coupling. Figure 10 exhibits the cross-correlation diagrams in the focused and defocused case for a simulated point target at an azimuth angle of $\alpha_o = 0^\circ$ and an elevation angle of $\varepsilon_o = 0^\circ$.

The overlap range of the two main lobes where angular measurements in elevation and azimuth are possible is highlighted. For the focused case (Fig. 10(a)) the correlation function exhibits a pronounced maximum at the position of the assumed object, whereas for the defocused case (Fig. 10(b)) a broadening of this maximum as a consequence of the above-mentioned ambiguity of the antenna diagram occurs making it difficult to exactly localize the angular position. Thus, according to these simulations, the performance of our concept utilizing two antennas severely depends on the mounting of these antennas in the focal plane of the dielectric lens.

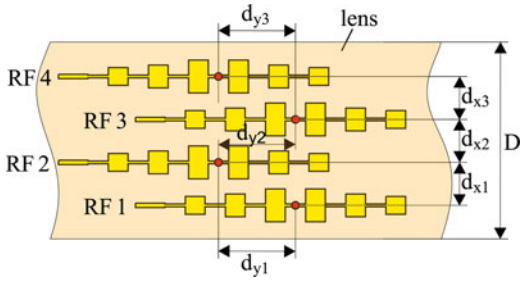

Fig. 11. Four-channel setup.

https://doi.org/10.1017/S1759078712000694 Published online by Cambridge University Press

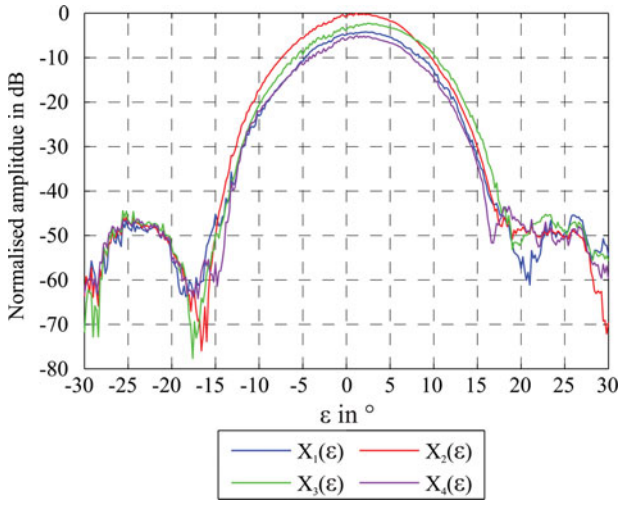

Fig. 12. Normalised measured two-way response in the *E*-plane.

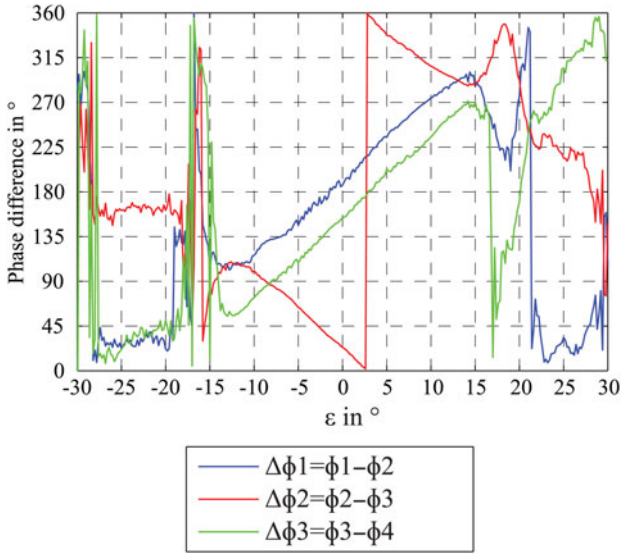

Fig. 13. Measured phase difference in the *E*-plane.

B) Four-channel configuration

In order to overcome the restraints of a two-channel configuration such as widening the field of view in combination with an improved angular accuracy or the capability to cope with multiple targets, our concept was extended to a four-antenna configuration as shown in Fig. 11. Hereby, the added outer beams exhibit only receive characteristics. Such a four-channel configuration possesses a higher degree of freedom with respect to the mutual displacement of the single antennas. The beam width can be adjusted with respect to the two planes by a proper design of the lens aperture and of the dimension of the planar antenna. The configuration proposed in Fig. 11 possesses a distinct advantage regarding the above described defocusing of the lens system. Figure 12 shows the measured two-way response of the system in the *E*-plane with all four receive channels. An angular displacement in elevation leads to a certain phase difference between antennas 1 and 2 (RF1 and RF2) and to a phase difference with opposite sign between antennas 2 and 3 (RF2 and RF3). Thus, this alternation of the sign of the phase difference (Fig. 13) is a signature for an angular displacement in elevation. As revealed in Fig. 8(b) an angular displacement in azimuth also results in a phase difference for the defocused case. However, as proven by simulations, this is not accompanied by this alternation of the sign of the phase difference. Thus, it is possible to distinguish between angular displacements in elevation and azimuth. In Fig. 14, the measured and simulated two-way response of the system in the *H*-plane is presented. The beam squint due to the quasi-optical offset of the feed antennas in this direction is clearly visible for all four receive beams.

In order to assess the angular accuracy of our antenna concept the CRLB (Cramer Rao Lower Bound) was applied [15] in the field of view of our sensor. An SNR of 25 dB was assumed in these calculations. In Fig. 15, the angular accuracy (standard deviation of angular estimation) is shown for angular estimations in azimuth (Fig. 15(b)) and elevation (Fig. 15(a)). In the proposed configuration, the angular accuracy is better than 0.2° in azimuth and better than 0.4° in

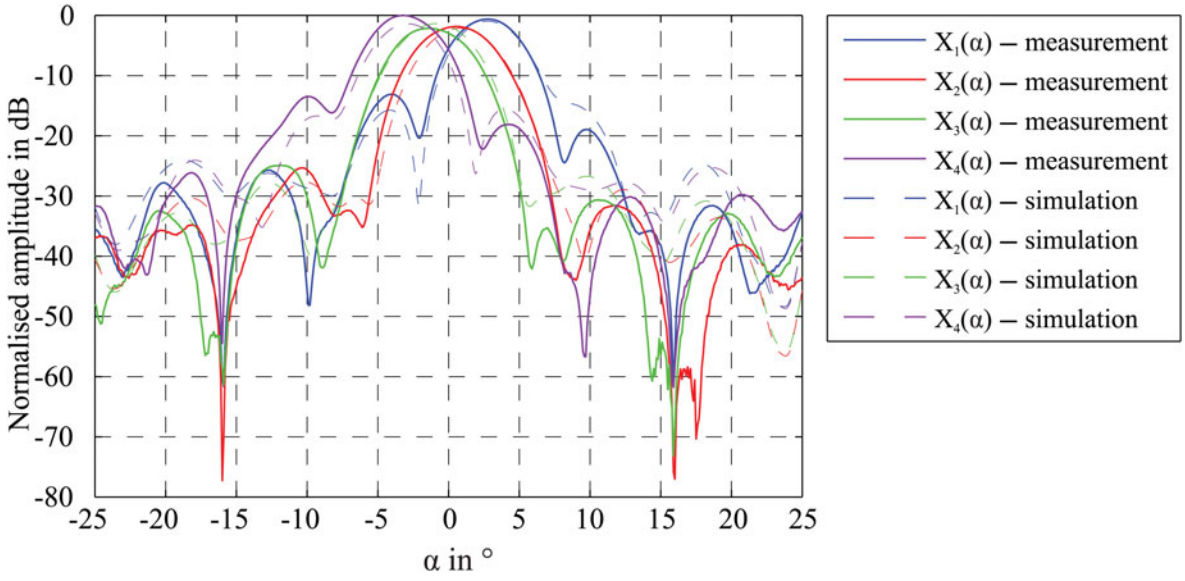

Fig. 14. Normalised measured and simulated two-way response in the *H*-plane.

https://doi.org/10.1017/S1759078712000694 Published online by Cambridge University Press

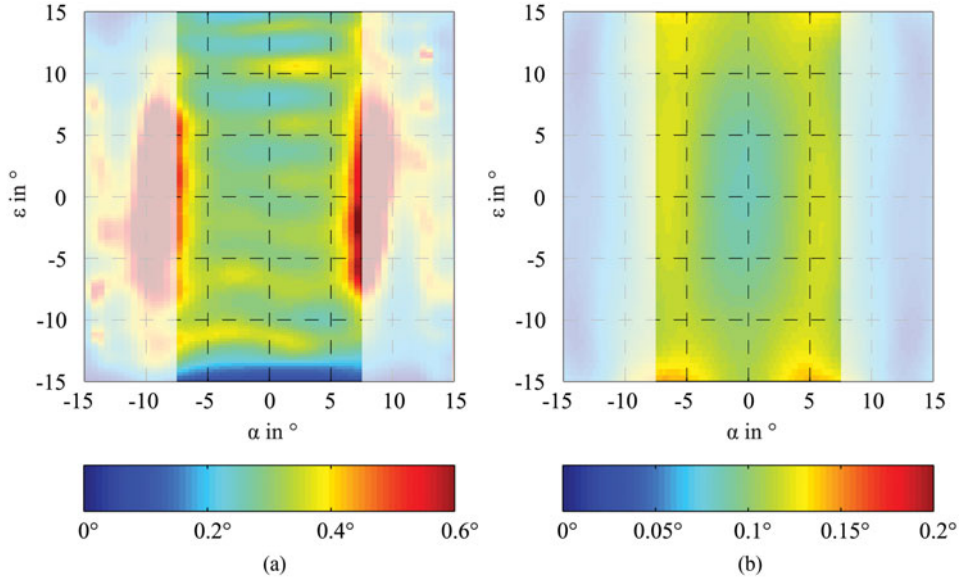

Fig. 15. Angular standard deviation in (a) elevation and (b) azimuth.

elevation within the field of view specified above. The angular resolution of our concept depends as primarily on the beam width for a conventional radar sensor and the associated signal processing for DOA.

V. CONCLUSIONS

In this contribution, an antenna concept consisting of a planar antenna array in combination with a cylindrical dielectric lens for angular estimations in azimuth and elevation was presented. The performance of a two-channel configuration deteriorates if the planar antennas are displaced with respect to the focal plane of the dielectric lens. However, a properly designed four-channel configuration exhibits a higher robustness regarding the mounting of the lens. Our antenna concept was integrated into a commercially available 77 GHz radar sensor and characterized. The performance of the proposed concept was evaluated using correlation algorithms and the CRLB. In order to validate the presented concept road testing especially in urban environments will be performed.

ACKNOWLEDGEMENTS

This work was supported by the German Federal Ministry of Education and Research (BMBF) within the project Radar on Chip for Cars (RoCC) in cooperation with the Robert Bosch GmbH. Dielectric lenses, the LRR3 radar architecture and helpful discussions were provided by the Robert Bosch GmbH, Stuttgart.

REFERENCES

[1] Li, H.; Rein, H.-M.; Suttorp, T.; Bock, J.: Fully integrated SiGe VCOs with powerful output buffer for 77 GHz automotive Radar systems and applications around 100 GHz. IEEE J. Solid-State Circuits, **39** (2004), 1650–1658.

[2] Forstner, H.P. et al.: A 77 GHz 4-channel automotive radar transceiver in SiGe, in Radio Frequency Integrated Circuits Symp., 2008, 233–236.

[3] Brunnbauer, M.; Meyer, T.; Ofner, G.; Mueller, K.; Hagen, R.: Embedded wafer level ball grid array (eWLB), in Electronic Manufacturing Technology Symp., Singapore, 2008, 994–998.

[4] Hasch, J.; Topak, E.; Schnabel, R.; Zwick, T.; Weigel, R., Waldschmidt, C.: Millimeter-wave technology for automotive radar sensors in the 77 GHz frequency band. IEEE Trans. Micro. Theory Tech., **60** (2012), 845–860.

[5] Sullivan, M.: Practical Array Processing, McGraw-Hill, New York, 2009.

[6] Hausz, W.; Zachary, R. A.: Phase-amplitude monopulse system. IRE Trans. Military Electron, **MIL-6** (2) (1962), 140–146.

[7] Diewald, F.; Klappstein, J.; Dickmann, J.; Dietmayer, K.: Radarinterferenzbasierte Höhenschätzung von Objekten des Fahrumfeldes, 4. Tagung Sicherheit durch Fahrerassistenz, 2010.

[8] Mayer, M.; Baur, K.; Walter, Th: Angular measurement with lens based automotive radar sensors, in Int. Radar Symp. IRS, Vilnius, Lithuania, 2010, 1–4.

[9] Volakis, J.: Antenna Engineering Handbook, 4th ed. McGraw-Hill, New York, 2007.

[10] Baur, K.; Mayer, M.; Binzer, Th.; Walter, Th.: Beamforming concepts for angular measurements in azimuth and elevation with 77 GHz lens based radar sensors, in Int. Microwave Symp., Baltimore, USA, 2011, 1–4.

[11] Goldsmith, P. F.: Quasioptical Systems: Gaussian Beam Quasioptical Propagation and Applications, John Wiley & Sons, New York, 1997.

[12] Hecht, E.: Optik, 3rd ed. Peter-Peregnius, London, 1991.

[13] Freundt, D.; Lucas, B.: LRR3 by Bosch – Long Range Radar Sensor for High-Volume Driver Assistance Systems Market, SAE, Detroit, USA, 2008.

[14] Baur, K.; Mayer, M.; Rack, V.; Vogel, D.; Walter, Th.: Angular measurements in azimuth and elevation using 77 GHz radar sensors, in European Radar Conf., Paris, France, 2010, 184–187.

https://doi.org/10.1017/S1759078712000694 Published online by Cambridge University Press

[15] Stoica, P.: MUSIC, maximum likelihood, and Cramer–Rao bound. IEEE Trans. Acoust. Speech Signal Process., **37** (5) (1989), 720–741.

Klaus Baur received his Dipl.-Ing. (FH) degree in mechatronic engineering from the University of Applied Sciences Ulm. He wrote his diploma thesis in the field of integration technologies for 77 GHz radar sensors in 2007. Since 2008, he has been working toward his Ph.D. at the University of Applied Sciences Ulm and the University of Erlangen-Nuremberg within the technology project Radar on Chip for Cars (RoCC) in close cooperation with the Robert Bosch GmbH. Since 2012, he has been with the Robert Bosch GmbH as a development engineer for 77 GHz automotive radar systems.

Marcel Mayer has graduated as a mechatronic engineer in 2007 at the University of Applied Sciences Ulm. From 2007 to 2011 he worked towards his Ph.D. at the University of Applied Sciences Ulm in the field of lens-based automotive radar sensors. He received his Dr.-Ing. from the University of Erlangen-Nuremberg in 2011. Since 2011, he has been with the Robert Bosch GmbH in Leonberg as a development engineer for driver assistance systems.

Steffen Lutz received the bachelor degree in mechatronics and the master degree in systems engineering from the University of Applied Sciences Ulm, Germany, in 2010 and 2011, respectively. Since 2011, he has been with the University of Applied Sciences in Ulm as research assistant. His research interests include array signal processing, MIMO radar systems, as well as RF system design.

Thomas Walter received his diploma degree and Ph.D. in electrical engineering from Stuttgart University, Germany. He then joined the corporate research of Bosch/Stuttgart working on microsystem technology and optical communication systems. In the business unit "driver assistance systems" of Bosch, Thomas Walter was responsible for the introduction of SiGe-MMICs into automotive radar sensors. Since 2005 he has been a professor for microelectronics and microsystem technology at the University of Applied Sciences Ulm, Germany. His main research interests include highly integrated automotive radar sensors and thin film solar cells.

https://doi.org/10.1017/S1759078712000694 Published online by Cambridge University Press